Soft Nanoscience Letters, 2019, 9, 1-16
http://www.scirp.org/journal/snl
ISSN Online: 2160-0740
ISSN Print: 2160-0600

Study on Enhanced Antibacterial and Cytotoxicity of Pure and Cadmium Doped Cerium Oxide against Gram-Positive and Gram-Negative Bacteria

Killivalavan Govindarasu[1], Kavitha Gnanasekaran[2], Sathyaseelan Balaraman[3*], Baskaran Iruson[4], Senthilnathan Krishnamoorthy[5], Rameshkumar Gubendiran[3], Babu Padmaraj[2], Elayaperumal Manikandan[6,7], Sivakumar Dhananjayan[8]

[1]Department of Physics, Bharathiar University, Coimbatore, India
[2]P. G. Research & Department of Physics, A. M. Jain College, Meenambakkam, India
[3]Department of Physics, University College of Engineering Arni (A Constituent College of Anna University Chennai), Arni, India
[4]Department of Physics Arignar Anna Govt. Arts College, Cheyyar, Tamil Nadu, India
[5]Department of Physics, VIT University, Vellore, India
[6]Department of Physics, Thiruvalluvar University, TUCAS Campus, Thennangur, India
[7]UNESCO UNISA Africa Chair in Nanosciences & Nanotechnology, College of Graduate Studies, University of South Africa, Muckleneuk Ridge, Pretoria, South Africa
[8]Department of Physics, Sree Krishna College of Engineering, Unai, Anai, India
Email: *bsseelan03@gmail.com

How to cite this paper: Govindarasu, K., Gnanasekaran, K., Balaraman, S., Iruson, B., Krishnamoorthy, S., Gubendiran, R., Padmaraj, B., Manikandan, E. and Dhananjayan, S. (2019) Study on Enhanced Antibacterial and Cytotoxicity of Pure and Cadmium Doped Cerium Oxide against Gram-Positive and Gram-Negative Bacteria. *Soft Nanoscience Letters*, **9**, 1-16.
https://doi.org/10.4236/snl.2019.91001

Received: December 26, 2018
Accepted: January 28, 2019
Published: January 31, 2019

Abstract

Pure and Cadmium (Cd) doped Cerium oxide nanoparticles (CeNPs) have been synthesised by the simple chemical co-precipitation technique. Cadmium ions of concentrations 1, 3 and 5 mol% were doped to investigate their influence on the structural and optical properties of CeO_2. The synthesised samples have been subjected to X-ray diffraction (XRD), scanning electron microscopy (SEM), energy dispersive X-ray (EDX) analysis and high-resolution transmission electron microscopy (HRTEM). The XRD and Raman patterns have witnessed the cubic structure of the cerium oxide nanoparticles. The average particle size of CeO_2 was found to be around 10 nm. SEM image has also ascertained that the grain size of pure CeO_2 appeared is bigger than that of the Cd-doped, which intern indicates the grain growth upon doping. Besides, the antibacterial activity of the cadmium doped cerium oxide nanoparticles against some human pathogens revealed that they have exhibited the maximum zone of inhibition against gram-positive bacteria than the gram-negative species. Further, the cytotoxic effect of Cd-doped CeO_2 sample is examined in cultured (MCF-7, A549 and Hep-2) cell.

Keywords

Co-Precipitation, XRD, SEM, HRTEM, Antibacterial Activity

1. Introduction

Of late, nanotechnology has been the primary focus, especially, on biomedical related research activities. It has been well demonstrated that the nanomaterial's exhibited several interesting properties and they were exploited in the field of life science research, biology and medicine [1]-[6]. Thus, these nanomaterials find a wide range of applications which include luminescent biomarkers, drug delivery systems, tissue engineering, etc [7]. Recently, owing to the enormous developments in nanoscience and nanotechnology, the field of nanomedicine plays an indispensable role to investigate the novel drugs to augment the conventional therapies, namely, surgical interventions, radiation and cytotoxic chemotherapy which are considerably effective in the cancer treatment [8] [9] [10] [11] [12]. It was reported that the Cerium oxide (CeO_2) and many rare earth metal oxides of lanthanide series were found to exhibiting face-centered cubic fluorite-type crystal structures. Cerium oxide nanoparticles (CeNPs) originated from the variable valence states (3+ and 4+) of cerium element. These nanoparticles could be explored for various applications in industrial areas such as the catalysts, polishing agents, fuel cells, ultraviolet absorbents in sunscreen lotions, gas sensors, etc. Its redox activity (Ce^{3+}/Ce^{4+} redox switch) along with the oxygen vacancies due to surface defects has led to various biological activities, namely, anti-inflammation, antiapoptotic, antioxidant property etc [13]. In literature, CeO_2 nanoparticles were prepared by several methods namely; hydrothermal synthesis [14], Co-precipitation technique [15] and Solvothermal Methods [16] [17]. Of these techniques, co-precipitation method is a quite simple process, low in cost, easy to prepare and industrially viable. In the present work, Cd-doped CeO_2 nanoparticles have been prepared using co-precipitation technique. The effect of Cadmium doping on the structural and morphological properties of CeO_2 has been studied using X-ray diffraction (XRD), Raman spectroscopy, SEM and HRTEM analysis. The biological activity against certain human pathogen was also analysed.

2. Materials and Method

2.1. Materials

Cadmium acetate (Cd $(CH_3COO)_2{\cdot}2H_2O$, Merck, pure), Cerium(III) Nitrate Hexahydrate $(Ce(NO_3)_3{\cdot}6H_2O$, Spectrochem, 99% purity), Sodium hydroxide (NaOH, Merck, 99.99% purity) and Polyethylene glycol (PEG) were taken as the initial reagents to synthesize the $Cd_{(1-x)}Ce_xO$ nanostructure. Deionized water was used as the solvent to prepare solutions of precursors.

2.2. Synthesis Procedure

In a typical synthesis process, appropriate quantities of $Cd(CH_3COO)_2{\cdot}2H_2O$ and $Ce(NO_3)_3{\cdot}6H_2O$ were grounded uniformly, mixed and finally dissolved in 350 ml distilled water with the assistance of continuous magnetic stirring. Measurable amount of Polyethylene glycol (PEG) and NaOH solution was then added into the above solution and the resulting one was kept under sonification for 30 minutes so as to achieve the pH value of 11. The prepared solution was then transferred into a Teflon-lined autoclave and heated at 100˚C for 22 hrs. The various compositions of the Cadmium substituted samples have been represented by a given formula $Cd_{(1-x)}Ce_xO$ with x being 0, 1.0, 3.0 and 5.0 mole percentage. The final products were obtained after washing and filtering several times with distilled water and anhydrous ethanol. Then it was dried at 100˚C in vacuum atmosphere.

2.3. Antibacterial Activity of Cd Doped CeO_2 NPs

The antibacterial activities of synthesized Cd doped CeO_2 NPs were studied against Gram-positive (G+ve) (*S. aureus*: *Staphylococcus aureus*) and Gram-negative (G−ve) (*E. col*: *Escherichia coli*, *P. aeruginosa*: *Pseudomonas aeruginosa*) strains by disk diffusion method. In brief, the bacterial strains were cultured in nutrient broth at 37˚C until the culture reached 1.5×10^8 colony forming units (CFU) per milliliter. About 20 mL of autoclaved molten nutrient agar was poured into the Petri dishes and allowed to cool. All of the bacterial cultures were swapped over solidified agar medium. Later, disks were loaded with Cd doped CeO_2 NPs solution of 20 μg/5μL through micropipette. The plates were incubated at 37˚C for 24 hours and the zones of inhibition (ZOIs) around the disks were measured.

2.4. Cell Culture and Cell Line Maintenance

Breast cancer cells (MCF-7), *Human Lung cancer cells* (A549) and *Human Larynx Carcinoma cancer cells* (Hep-2) were obtained. Then, these cell lines were grown as a monolayer in Dulbecco's modified Eagle's medium (DMEM: Himedia Laboratories, Mumbai, India), medium which was supplemented with 10% fetal bovine serum , 100 U/mL penicillin, and 100 μg/mL streptomycin (Hi Media Laboratories Mumbai, India) cells grown at 37˚C in incubator under 5% CO_2 with high humidity [18] [19] [20].

2.5. MTT Assay Method for Evaluation of Cell Viability and Cytotoxicity

The anticancer activity of samples on MCF-7, A549 and Hep-2 cells was determined by the MTT (3-(4, 5-*dimethyl thiazol*-2*yl)*-2, 5-*diphenyl tetrazolium bromide*) assay was used to assess the cytotoxicity by Mosmann [21] [22]. There Cells (1×10^5/well) were plated in 0.2 ml of the cells with concentration of 1×10^5 cells/ml were plated in well 96-well plates. The plates were incubated for 24

hrs in 5% CO_2 incubator for cytotoxicity. After incubation, normal breast (MCF-7, A549 and Hep-2) cells were cultured in 1:1 mixture of *dimethyl sulfoxide* (DMSO). Then, they were added to each well and mixed well by micropipette [23]. The percentage of viable cells was visualized by the development of purple color due to formation of formazan crystals. The suspension was transferred to the cuvette of a spectrophotometer and observed significant variance/instability in the optical density (OD). Measurements were performed and the concentration required for a 50% inhibition of viability (IC_{50}) was determined and used for the bioassays.

2.6. Morphological Cross Section of Apoptotic Cells by Acridine Orange (AO) and Ethidium Bromide (EB) Staining

The cross sectional morphology of apoptotic cells was carried by AO/EB double staining method which was proposed by Spector *et al*. [24]. The cells were treated with IC_{50} Concentration of Cd doped CeO_2 for 24 hours in a humidified atmosphere of 5% CO_2 at 37˚C incubation. The cells were harvested and washed with cold PBS. Cell pellets were diluted with PBS concentration of 5×10^6 cells/mL and mixed with 10 µl of AO/EB solution (3.8 µM of AO and 2.5 µM of EB in PBS). The cross-section morphology of apoptotic was investigated by fluorescence microscope (Carl Zeiss, Axioscope 2 plus) with UV (450 - 490 nm) [25].

2.7. Morphological Cross Section of Apoptotic Cells by DAPI Staining

In addition to the above study, the morphological cross-section of apoptotic cells was also examined by DAPI staining. 4',6-*diamidino*-2-*phenylindole* (DAPI) staining was carried out according to the method described by Papi *et al*. with some modifications [26]. Hep-2 cells were grown on sterile glass slides overnight and treated for 48 hours with sulforaphene (in serum free media) concentration of IC_{50} (33.8 µM). The cells were incubated for 48 hours in a humidified atmosphere of 5% CO_2 at 37˚C. At the end of the incubation, cells were fixed with 4% paraformaldehyde and then *phosphate buffered saline* (0.1% in PBS). Cells were finally stained using DAPI in PBS (2.5 µg/mL) and allowed to stand for 20 min in a dark condition. Finally, morphological cross-section reforms were observed by fluorescence microscopy. (Magnification × 400) (Zeiss, Oberkochen, Germany) [27].

2.8. Characterization of Cd Doped CeO_2 NPs

Powder X-ray diffraction (XRD) measurements were carried out for pure and cadmium doped CeO_2 samples using a Bruker D8 advance diffractometer with monochromatized Cu Kα radiation (λ = 1.5418 Å). The X-ray source was operated at 40 kV with a current of 40 mA. The measurements were performed by $\theta/2\theta$ scans in the 2θ range from 20˚ to 80˚ with a step size of 0.02˚ and at a scan rate of 2˚/min. The micrographs of cadmium doped CeO_2 samples were also

obtained using the scanning electron microscope (Model: JEOL-JSM 6360) and high-resolution transmission electron microscope-HRTEM (Model: JEOL/JEM 2100). Elemental analysis was carried out for ascertaining the concentrations of cadmium in CeO_2 materials with the aid of energy dispersive X-ray spectroscopy equipped with scanning electron microscopy. Micro-Raman spectra were recorded in backscattering configuration and analyzed using a JobinYvon T64000 spectrometer equipped with the nitrogen cooled charge-coupled-device detector. The normal and apoptotic cells have been visualised using an upright fluorescent microscope (Nikon Eclipse, Inc., Japan) at 40× magnification with the excitation filter at 510 - 590 nm.

3. Results and Discussion

3.1. X-Ray Diffraction (XRD) Analysis on Pure and Cd Doped CeO_2

XRD patterns of pure and Cd doped CeO_2 nanoparticles at different concentrations of Cd (1, 3 and 5 mol%) are shown in Figure 1. The structural properties of the pure and Cd doped CeO_2 nanoscale materials were determined through XRD measurements. The synthesized product exhibits the diffraction peaks with parallel planes (hkl) which indicate the presence of CeO_2 compound with cubic

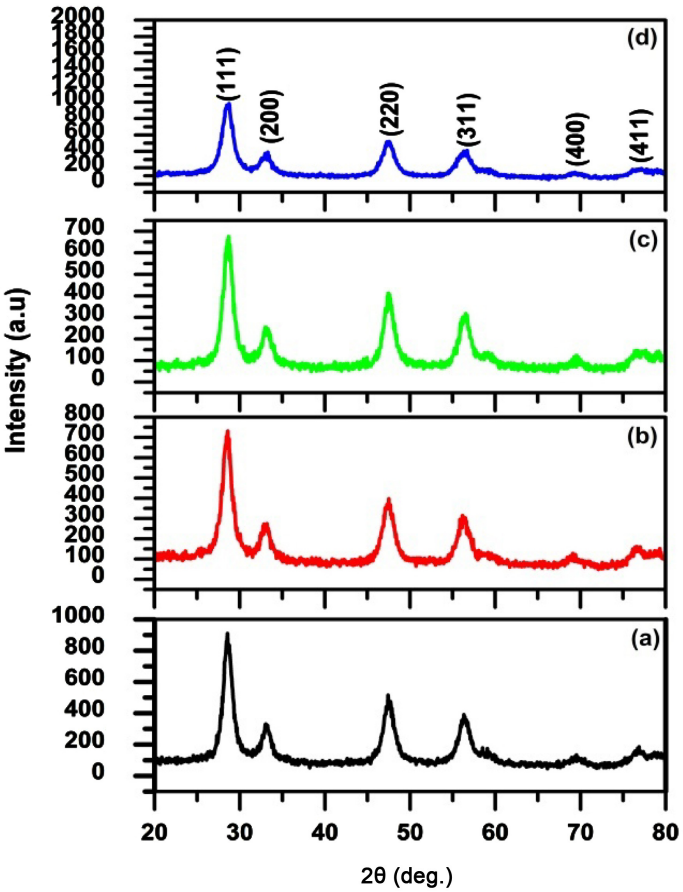

Figure 1. XRD patterns of the CeO_2 nanoparticles containing: (a) 0%, (b) 1.0%, (c) 3.0%, and (d) 5.0% of Cd.

NaCl structure (JCPDS card number: 34-0394). The intensities of (111), (200), (220), (311), (400) and (411) peaks in the 1, 3 and 5% Cd added CeO_2 were found to be prominent. It can be seen from the XRD pattern that the positions of the peaks have been shifted towards the higher 2θ value with increase in "Cd" content. In **Figure 1**, the "d" values are calculated using (111) peak for different concentration of Cd ions doped in CeO_2 matrix. The $d_{(111)}$ values are found to decrease with the Cd content. Thus, the decreasing trend of $d_{(111)}$ values reflects that lattice parameters decrease with Cd doping which is in good agreement with the earlier reported results [28] [29] [30]. XRD results also provide a clue that the Cd ions replace some of the Ce ions in the CeO_2 matrix and ruled out the formation of any other crystalline phase. The average crystalline sizes of the pure and Cd-doped CeO_2 have been found in the range of 20 - 42 nm using Scherrer's equation [31].

$$D = 0.89\lambda/(\beta\cos\theta). \quad (1)$$

Here θ is the Bragg diffraction angle, β is the peak width at half maxima. The broadening of the diffraction peaks with increase in the concentration of dopant reveals the formation of nanocrystals with the phase CeO_2.

3.2. Raman Studies on Pure and Cd Doped CeO_2 NPs

Figure 2 shows the Raman spectra of the pure and Cd (0, 1, 3 and 5 mol%) doped CeO_2 nanoparticles in the frequency range 200 - 1200 cm^{-1}. The CeO_2 exhibited a strong Raman spectrum at 455 cm^{-1} because of the F_{2g} Raman active mode of the fluorite structure [32]. It also exhibits a shoulder like scattering vibrations at ≈ 602 cm^{-1} and 1050 cm^{-1} owing to the normal Raman inactive (IR active) transverse and longitudinal optical phonon modes, respectively, at the Brillouin zone center [33]. The spectrum of Cd doped CeO_2 showed the prominent peaks at 452 cm^{-1} and a weak band 602 cm^{-1}, 1043 cm^{-1}. The band at 452 cm^{-1} represents the triply degenerate F_{2g} mode and it is identified as a symmetric breathing mode of the O atoms around Ce ions [34]. The weak band observed near 602 and 1043 cm^{-1} could be attributed to a non-degenerate longitudinal optical (LO) mode of CeO_2 [35].

3.3. SEM Analysis on Pure and Cd Doped CeO_2 NPs

Figures 3(a)-(d) represent the overall surface morphology of pure and Cd doped CeO_2 nanoparticles. The figures reveal that the pure CeO_2 compound consists of large aggregates transformed to more fine aggregates up on increasing the concentration of dopant. The images also show the agglomeration of homogeneous particles with a size distribution of around 1μm in diameter. **Figure 4** shows the EDX spectrum of Cd doped CeO_2 and it confirms the presence of Cd ions in the CeO_2 matrix. Further, the estimated compositions do exist in the sample in respect of Cadmium, cerium and oxygen elements. The atomic % of Cd, Ce, and O are 1.20, 24.45 and 74.35, respectively, for 3% of Cd doping.

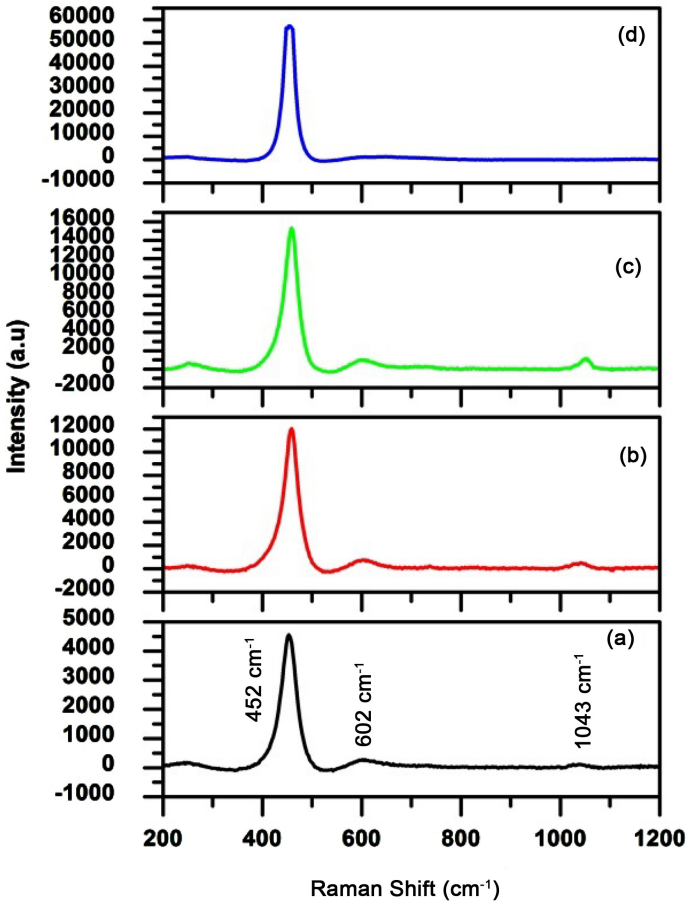

Figure 2. Raman spectra of the CeO_2 nanoparticles containing: (a) 0%, (b) 1.0%, (c) 3.0%, and (d) 5.0% of Cd.

3.4. HRTEM Analysis on Pure and Cd Doped CeO_2 NPs

HRTEM images of the samples shown in **Figure 5(a)** and **Figure 5(c)** provide the average crystalline size for pure and doped CeO_2 and it confirms that the average crystalline size of Cd doped nanoparticles is smaller than that of pure CeO_2. The particle size of pure and Cd doped CeO_2 is 6 nm and 5 nm, respectively. The results are in good agreement with XRD data. It was observed that size of particles decreases with increase of dopant concentrations. **Figure 5(b)** and **Figure 5(d)** depicts SAED patterns of CeO_2 and Cd doped CeO_2 and it confirms the fluorite structure of CeO_2 and the ring patterns showed (111), (200), (220) and (311) planes of cubical unit cell.

3.5. Antibacterial Analysis of Cd Doped CeO_2 NPs

The antibacterial assay was performed against G+ve and G−ve bacterial entities using Cd doped CeO_2 NPs sample loaded at a concentration of 20 μg/05μL on disks. **Figure 6** and **Figure 7** reflect the measurements in size of ZOI around Cd doped CeO_2 NPs poured disks. The synthesized Cd doped CeO_2 NPs have proven efficiency and comparatively low genotoxic and cytotoxic behavior toward healthy cells, when compared to Cd doped CeO_2 NPs synthesized by

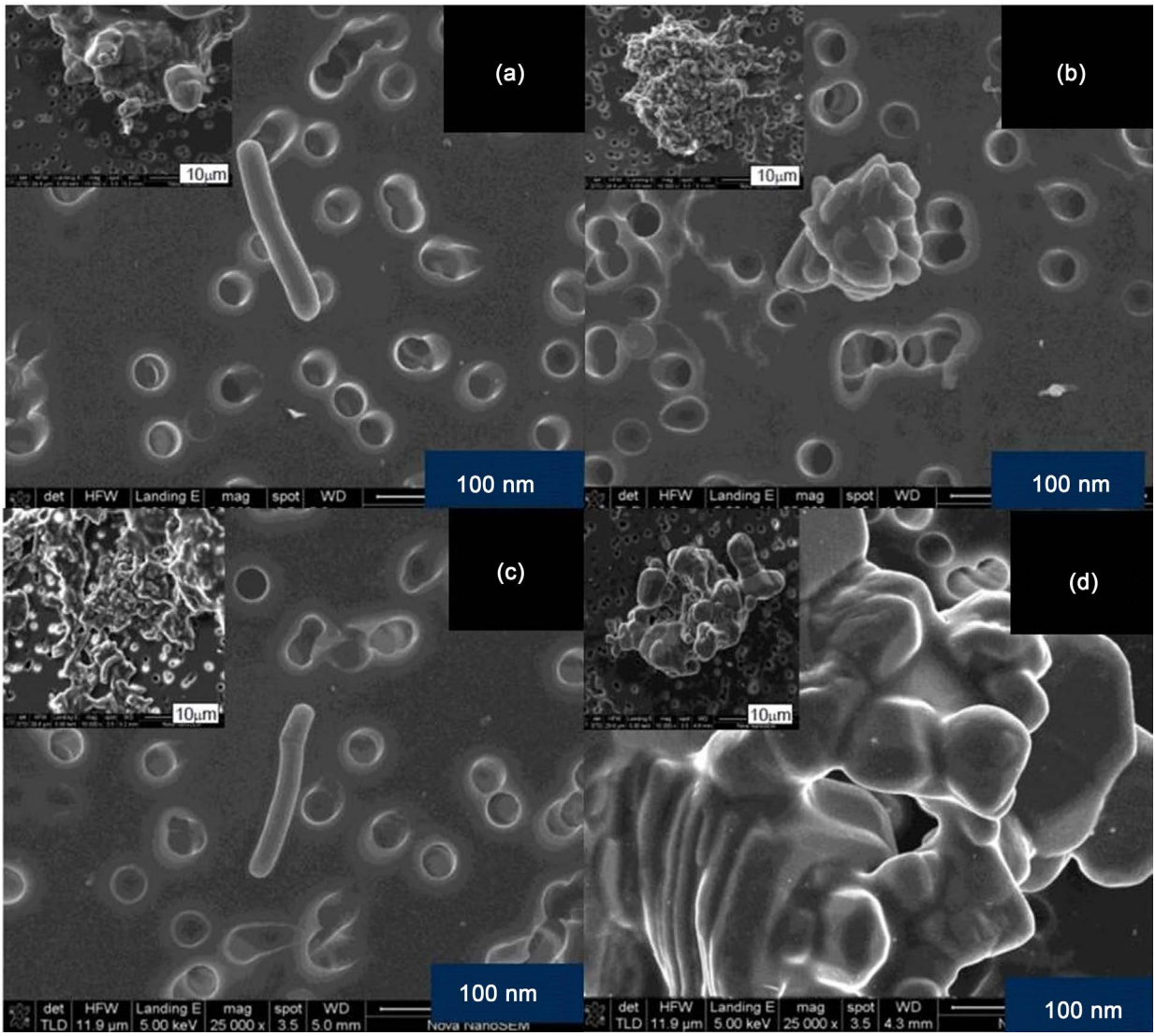

Figure 3. SEM images of pure and doped CeO_2 (a) Pure CeO_2, (b) 1% Cd, (c) 3% Cd, (d) 5% Cd.

various chemical methods [36] [37] [38].

3.6. Cytotoxicity Analysis of MCF-7, A549 and Hep2 Cell Line

The cytotoxic effect of Cd doped CeO_2 NPs was examined in cultured (MCF-7, A549 and Hep-2) cell line by exposing cells for 72 hours. The cultured medium of Cd doped CeO_2NPs led to inhibition at the various concentrations (10 to 100 μg/ml as shown in **Figure 8**. The cancer cell viability is decreased partially with increasing the concentration of Cd doped CeO_2 NPs. The results show the dose-response relationship with tested cells only at higher concentrations, but there is no significant toxicity [39].

3.7. Morphological Cross Section of Apoptotic Cells by DAPI Staining and AO/EtBr Double Staining

Acridine orange (AO)/Ethidium Bromide (EtBr) staining and DAPI staining

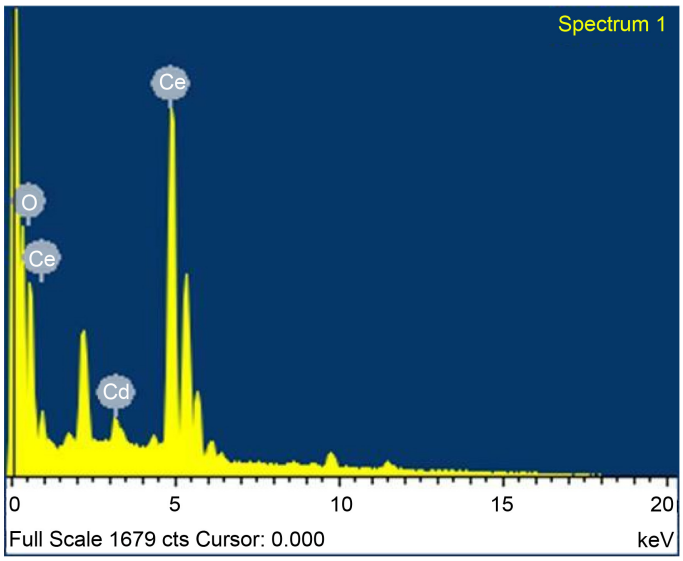

Figure 4. EDX analysis of 5% Cd doped CeO_2.

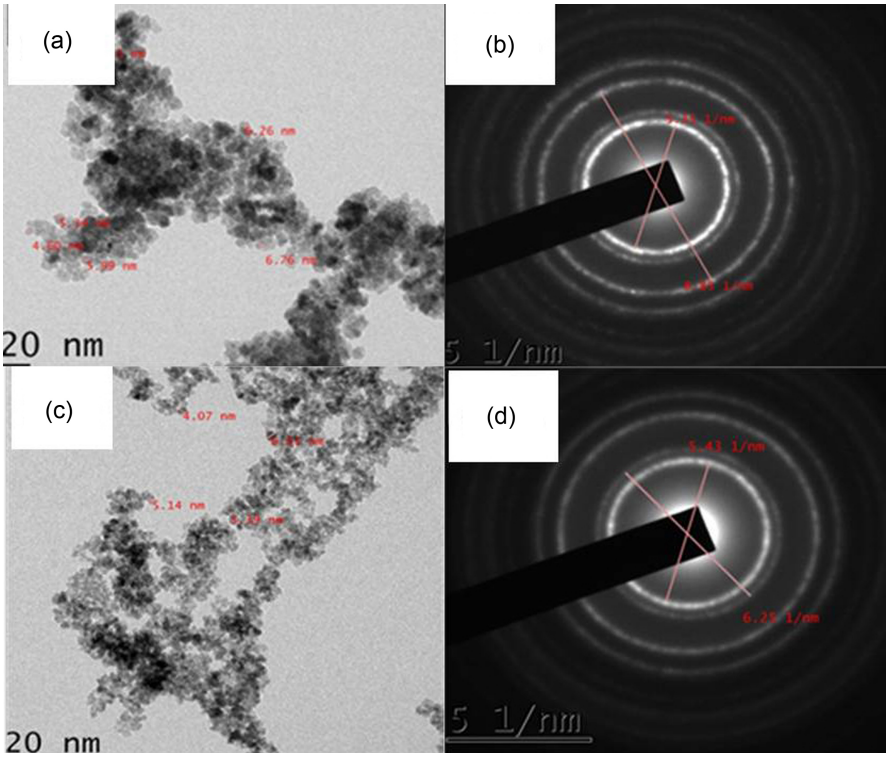

Figure 5. HRTEM images of pure and doped CeO_2. (a) Pure CeO_2, (b) SAED pattern of pure CeO_2, (c) 3% cd, and (d) SAED pattern of cd doped CeO_2.

methods were utilized to study morphological evidence of apoptosis on the Cd doped CeO_2 treated cells. From **Figure 9**, it is very clear that the apoptosis was noticed with the morphological changes in the cell shape. Points at that there morphological change are because of the activation of caspase cascades. We found that the cells were regular in morphology and they have grown fully in patches in the control group. However, after the treatment, the cells started

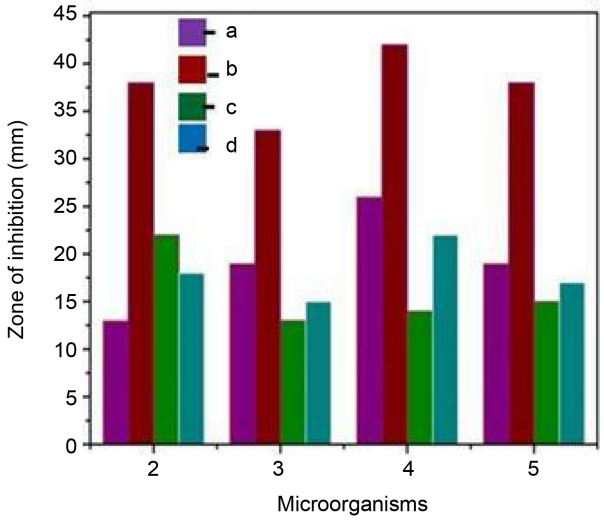

Figure 6. Antibacterial activity of CeO_2 NPs containing: (a) Pure, (b) 1.0%, (c) 3.0%, and (d) 5.0% of Cd.

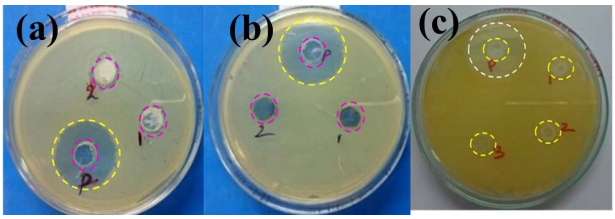

Figure 7. Zone of inhibition values for different concentration doped CeO_2 NPs containing: Gram-positive [*S. aureus* (a)] and Gram-negative [*E. coli* (b), *P. aeruginosa* (c)] Pure (P), 1.0% (1), 3.0% (2), and 5.0% (3) of Cd.

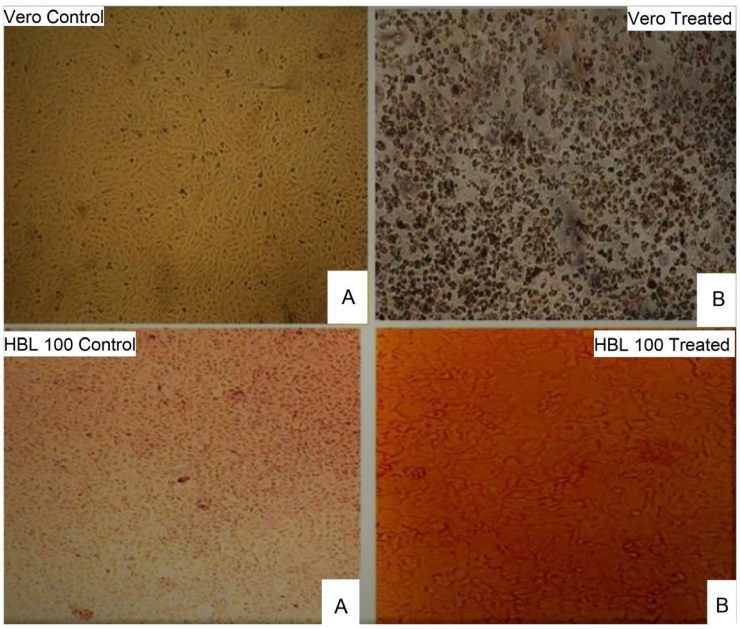

Figure 8. Vero and HBL 100 cell lines: (A) Control Cells. (B) Cd doped CeO_2 NPs Treated at the cell lines.

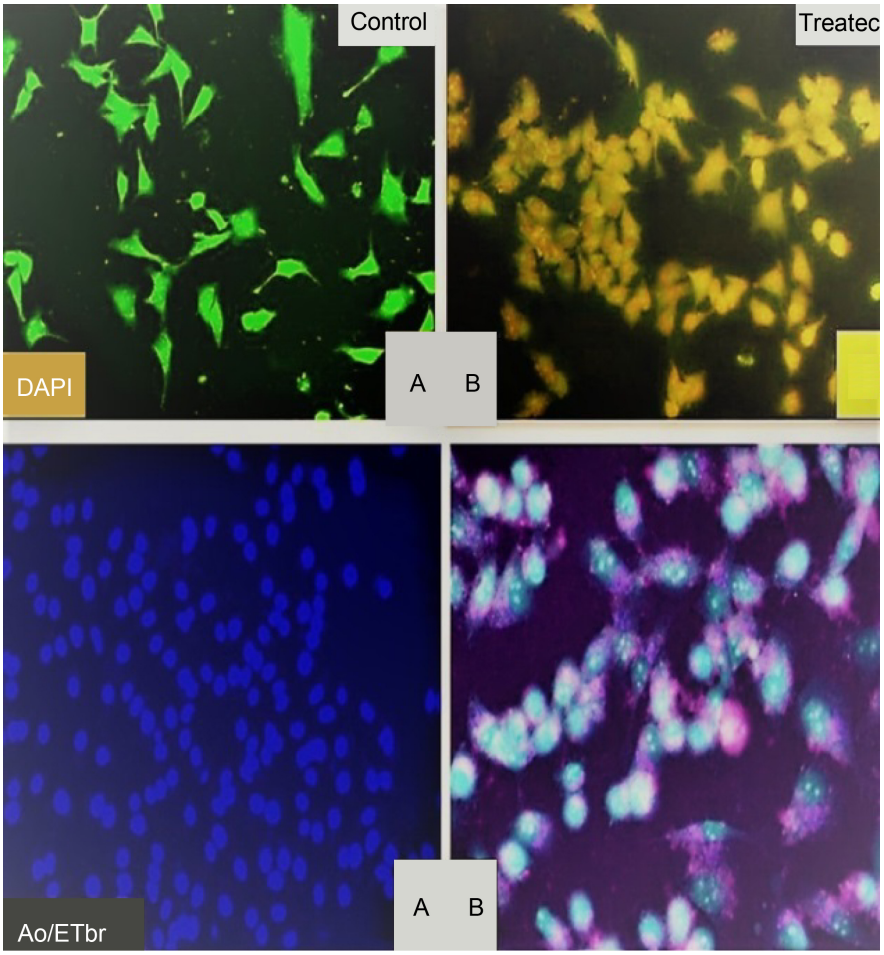

Figure 9. Cells treated with (A) control (B) Cd doped CeO_2 NPs at the respective IC_{50} concentrations and the morphologies Observed after staining with DAPI and Ao/EtBr.

exhibiting the apoptotic characteristics of nuclear condensation, cell shrinkage and fragmentation [40]. Further, the DAPI staining also revealed an increase in the number of apoptotic treated cells in terms of both nuclear condensation and cell structure loss [41] [42] [43]. Cd-doped CeO_2 nanoparticles possess a fair control of the pathogenic activity. The cytotoxicity activity of Cd-doped CeO_2 was also assessed for the cell lines MCF-7, A549 and Hep2 and the typical IC_{50} values are tabulated in **Table 1**. The obtained values have been compared with literature values reported for HT29 and SW620 cells using pure CeO_2 nanoparticles.

The cytotoxic effects of pure and Cd-doped CeO_2 nanoparticles suggest that they can be used for the development of drugs against colorectal cancer. The apoptotic potential CeO_2 nanoparticles upon doping with Cd ions were studied in breast cancer cell line MCF-7. A characteristic change in chromatic condensation and nuclear fragmentation has been observed which indicates the mechanism of cell death induced by the Cd-doped CeO_2 NPs. A similar kind of study made for pure CeO_2 NPs for HT29 cells [44] in the expression levels of Bcl2 and BclxL proteins. In both cases, it has been confirmed that nanoparticles of CeO_2

Table 1. Cytotoxicity of Cd-doped CeO_2 in MCF-7, A549 and Hep2 cells.

Sl. No.	Compound	Cell lines	IC_{50} values
1	CeO_2 NPs	MCF-7 A549 Hep2	47.6 48.2 (present work) 47.1
2	Cd doped CeO_2 NPs	MCF-7 A549 Hep2	70 µg/ml 70 µg/ml (present work) 70 µg/ml
3	CeO_2 NPs	HT29 SW620	50 µg/ml [36]

have the capacity of reducing cell proliferation.

4. Conclusion

Nanocrystalline forms of cerium oxide and cadmium doped cerium oxide have been successfully synthesized using chemical precipitation method. From XRD analysis, it was ascertained that the incorporation of cadmium ions did not alter the unit cell structure of CeO_2 for all concentrations of dopant's viz 1%, 3% and 5%. As per Debye-Scherrer's calculations, the average particle size of Cd-doped CeO_2 was estimated to be in the range 8 - 10 nm. Raman spectrum of Cd-doped CeO_2 showed that no new bands formed due to the dopant ions. This implied that the possible modes of scattering vibrations for fluorite type of cubic structure could also be seen in the Cd-doped CeO_2 which in turn reciprocates the results obtained from XRD. SEM-EDAX measurements revealed the actual compositions of cadmium ions in the CeO_2 matrix. Dopant has also influenced in transforming large aggregate particles into fine ones. However, agglomeration is also observed in doped samples as that of pure CeO_2. HRTEM analysis on pure and Cd-doped CeO_2 brings out the fact that the decrease in the particle size upon an increase in the dopant concentration. SAED patterns provide additional confirmation of restoration crystal structure by CeO_2 matrix even after doping. The minimal inhibitory concentration (MIC) behaviour of Cd-doped CeO_2 nanoparticles has been assessed using gram-positive and gram-negative bacteria.

Conflicts of Interest

The authors declare that there is no conflict of interests regarding the publication of this manuscript.

References

[1] Wang, Y., Zi, XY., Su, J., Zhang, H.X., Zhang, X.R., Zhu, H.Y., Li, J.X., Yin, M., Yang, F. and Hu, Y.P. (2012) Cuprous Oxide Nanoparticles Selectively Induce Apoptosis of Tumor Cells. *International Journal of Nanomedicine*, **7**, 2641-2652.

[2] Yang, F., Tang, Q., Zhong, X., Bai, Y., Chen, T., Zhang, Y., Li, Y. and Zheng W. (2012) Surface Decoration by Spirulina Polysaccharide Enhances the Cellular Uptake and Anticancer Efficacy of Selenium Nanoparticles. *International Journal of*

Nanomedicine, **7**, 835-844.

[3] Lee, P., Zhang, R., Li, V., Liu, X., Sun, R.W.Y., Che, C.-M. and Wong, K.K.Y. (2012) Enhancement of Anticancer Efficacy Using Modified Lipophilic Nanoparticle Drug Encapsulation. *International Journal of Nanomedicine*, **7**, 731-737.

[4] Murphy, E.A., Majeti, B.K., Barnes, L.A., Makale, M., Weis, S.M., Lutu-Fuga, K., Wrasidlo, W. and Cheresh, D.A. (2008) Nanoparticle-Mediated Drug Delivery to Tumor Vasculature Suppresses Metastasis. *Proceedings of the National Academy of Sciences*, **105**, 9343-9348. https://doi.org/10.1073/pnas.0803728105

[5] Siddiqui, I.A., Adhami, V.M., Chamcheu, J.C. and Mukhtar, H. (2012) Impact of Nanotechnology in Cancer: Emphasis on Nanochemoprevention. *International Journal of Nanomedicine*, **7**, 591-605. https://doi.org/10.2147/IJN.S26026

[6] Ghadiali, J.E., Cohen, B.E. and Stevens, M.M. (2010) Protein Kinase-Actuated Resonance Energy Transfer in Quantum Dot-Peptide Conjugates. *American Chemical Society Nano*, **4**, 4915-4919. https://doi.org/10.1021/nn101293s

[7] Wason, M.S. and Zhao, J. (2013) Cerium Oxide Nanoparticles: Potential Applications for Cancer and Other Diseases. *American Journal of Translational Research*, **5**, 126-131.

[8] Lee, S.K., Kim, G.S., Wu, Y., Kim, D.J., Lu, Y., Kwak, M., Han, L., Hyung, J.H., Seol, J.K., Sander, C., Gonzalez, A., Li, J. and Fan, R. (2012) Nanowire Substrate-Based Laser Scanning Cytometry for Quantitation of Circulating Tumor Cells. *Nano Letters*, **12**, 2697-2704. https://doi.org/10.1021/nl2041707

[9] Dicheva, B.M., ten Hagen, T.L., Li, L. Schipper, D., Seynhaeve, A.L., van Rhoon, G.C., Eggermont, A.M., Lindner, L.H. and Koning, G.A. (2013) Cationic Thermosensitive Liposomes: A Novel Dual Targeted Heat-Triggered Drug Delivery Approach for Endothelial and Tumor Cells. *Nano Letters*, **13**, 2324-2331. https://doi.org/10.1021/nl3014154

[10] Kanapathipillai, M., Mammoto, A., Mammoto, T., Kang, J.H., Jiang, E., Ghosh, K., Korin, N., Gibbs, A., Mannix, R. and Ingber, D.E. (2012) Inhibition of Mammary Tumor Growth Using Lysyl Oxidase-Targeting Nanoparticles to Modify Extracellular Matrix. *Nano Letters*, **12**, 3213-3217. https://doi.org/10.1021/nl301206p

[11] Zhao, G. and Rodriguez, B.L. (2013) Molecular Targeting of Liposomal Nanoparticles to Tumor Microenvironment. *International Journal of Nanomedicine*, **8**, 61-71.

[12] Wang, Y., Yang, F., Zhang, H.X., Zi, X.Y., Pan, X.H., Chen, F., Luo, W.D., Li, J.X., Zhu, H.Y. and Hu, Y.P. (2013) Cuprous Oxide Nanoparticles Inhibit the Growth and Metastasis of Melanoma by Targeting Mitochondria. *Cell Death and Disease*, **4**, 783. https://doi.org/10.1038/cddis.2013.314

[13] Heckert, E.G., Karakoti, A.S., Seal, S. and Self, W.T. (2008) The Role of Cerium Redox State in the SOD Mimeticactivity of Nanoceria. *Biomaterials*, **29**, 2705-2709. https://doi.org/10.1016/j.biomaterials.2008.03.014

[14] Hirano, M. and Kato, E. (1996) Hydrothermal Synthesis of Cerium (IV) Oxide. *Journal of the American Ceramic Society*, **79**, 777-780. https://doi.org/10.1111/j.1151-2916.1996.tb07943.x

[15] Sathyaseelan, B., Sambasivam, S., Alagesan, T. and Sivakumar, K. (2014) *Ex-Situ* Studies on Calcinations of Structural, Optical and Morphological Properties of Post-Growth Nanoparticles CeO_2 by HRTEM and SAED. *International Journal of Nano Dimension*, **5**, 341-349. https://doi.org/10.7508/IJND.2014.04.005

[16] Kaviyarasu, K., Manikandan, E., Nuru, Z.Y. and Maaza, M. (2017) Synthesis and Characterization Studies of Pb:Zr:/O_2 Nanorods for Optoelectronic Applications.

Journal of Nanomaterials & Molecular Nanotechnology, **3**, 10-80.

[17] Kaviyarasu, K., Fuku, X., Mola, G.T., Manikandan, E., Kennedy, J. and Maaza, M. (2016) Photoluminescence of Well-Aligned ZnO Doped CeO_2 Nanoplatelets by a Solvothermal Route. *Materials Letters*, **183**, 351-354. https://doi.org/10.1016/j.matlet.2016.07.143

[18] Chauhan, S. and Upadhyay, M.K. (2012) Fruit Based Synthesis of Silver Nanoparticles—An Effect of Temperature on the Size of Particles. *Recent Research in Science and Technology*, **4**, 41-44.

[19] Bhowmik, D., Sampath Kumar, K.P., Yadav, A., Shweta, S., Paswan, S. and Amit Sankar, D. (2012) Recent Trends in Indian Traditional Herbs *Syzygium aromaticum* and Its Health Benefits. *Journal of Pharmacognosy and Phytochemistry*, **1**, 13-22.

[20] Inbathamizh, L., Mekalai Ponnu, T. and Janancy Mary, E. (2013) *In Vitro* Evaluation of Antioxidant and Anticancer Potential of *Morinda pubescens* Synthesized Silver Nanoparticles. *Journal of Pharmacy Research*, **6**, 32-38. https://doi.org/10.1016/j.jopr.2012.11.010

[21] Mosmann, T. (1983) Rapid Calorimetric Assay for Cellular Growth and Survival: Application to Proliferation and Cytotoxicity Assays. *Journal of Immunological Methods*, **65**, 55-63. https://doi.org/10.1016/0022-1759(83)90303-4

[22] Krishnaraj, C., Jagan, E.G., Rajasekar, S., Selvakumar, P., Kalaichelvan, P.T. and Mohan, N. (2010) Synthesis of Silver Nanoparticles Using *Acalypha indica* Leaf Extracts and Its Antibacterial Activity against Water Borne Pathogens. *Colloids and Surfaces B*: *Biointerfaces*, **76**, 50-56. https://doi.org/10.1016/j.colsurfb.2009.10.008

[23] Kroemer, G., Zamzami, N. and Susin, S.A. (1997) Mitochondrial Control of Apoptosis. *Immunology Today*, **18**, 44-51. https://doi.org/10.1016/S0167-5699(97)80014-X

[24] Spector, D.L., Goldman, R.D. and Leinwand, L.A. (1998) Cells: A Laboratory Manual. Cold Spring Harbor Laboratory, New York.

[25] Krishnaraj, C., Muthukumaran, P., Ramachandran, R., Balakumaran, M.D. and Kalaichelvan, P.T. (2014) *Acalypha indica* Linn: Biogenic Synthesis of Silver and Gold Nanoparticles and Their Cytotoxic Effects against MDA-MB-231, Human Breast Cancer Cells. *Biotechnology Reports*, **4**, 42-49. https://doi.org/10.1016/j.btre.2014.08.002

[26] Papi, A., Farabegoli, F., Iori, R., Orlandi, M., De Nicola, G.R., Bagatta, M., Angelino, D., Gennari, L. and Ninfali, P. (2013) Vitexin-2-O-Xyloside, Raphasatin and (−)-Epigallocatechin-3-Gallate Synergistically Affect Cell Growth and Apoptosis of Colon Cancer Cells. *Food Chemistry*, **138**, 1521-1530. https://doi.org/10.1016/j.foodchem.2012.11.112

[27] Inbathamizh, L., Mekalai Ponnu, T. and Janancy, M. (2013) *In Vitro* Evaluation of Antioxidant and Anticancer Potential of *Morinda pubescens* Synthesized Silver Nanoparticles. *Journal of Pharmacy Research*, **6**, 32-38. https://doi.org/10.1016/j.jopr.2012.11.010

[28] Qi, Y., Wen, H., Zhang, W., Song, Y.Q., Yang, Q.H., Zhu, H. and Xiao, J.Q. (2007) Room-Temperature Ferromagnetism in Pure and Co Doped CeO_2 Powders. *Journal of Physics*: *Condensed Matter*, **19**, Article ID: 246205.

[29] Kumar, S., Kim, Y.J., Koo, B.H. and Lee, C.G. (2009) Structural and Magnetic Properties of Co Doped CeO_2 Nano-Particles. *IEEE Transactions on Magnetics*, **45**, 2439-2441. https://doi.org/10.1109/TMAG.2009.2018602

[30] Thurber, A., Reddy, K.M., Shutthanandan, V., Engelhard, V.H., Wang, C., Hays, J. and Punnoose, A. (2007) Ferromagnetism in Chemically Synthesized CeO_2

Nanoparticles by Ni Doping. *Physical Review B*, **76**, Article ID: 165206. https://doi.org/10.1103/PhysRevB.76.165206

[31] Plug, H.P. and Alexander, L.E. (1954) X-Ray Diffraction Procedures for Polycrystalline and Amorphous Material. Wiley, New York.

[32] Arias, M.A., Garcia, F.M., Salamanca, L.N., Valenzuela, R.X., Conesa, J.C. and Soria, J. (2000) Structural and Redox Properties of Ceria in Alumina-Supported Ceria Catalyst Supports. *The Journal of Physical Chemistry B*, **104**, 4038-4046. https://doi.org/10.1021/jp992796y

[33] Shyu, J.Z., Weber, W.H. and Gandhi, H. (1988) Surface Characterization of Alumina-Supported Ceria. *The Journal of Physical Chemistry*, **92**, 4964-4970. https://doi.org/10.1021/j100328a029

[34] Lin, X.M., Li, L.P., Li, G.S. and Su, W.H. (2001) Transport Property and Raman Spectra of Nanocrystalline Solid Solutions $Ce_{0.8}Nd_{0.2}O_{2-\delta}$ with Different Particle Size. *Materials Chemistry and Physics*, **69**, 236-240. https://doi.org/10.1016/S0254-0584(00)00409-0

[35] Weber, W.H., Hass, K.C. and McBride, J.R. (1993) Raman Study of CeO_2: Second-Order Scattering, Lattice Dynamics, and Particle-Size Effects. *Physical Review B*, **48**,178-185. https://doi.org/10.1103/PhysRevB.48.178

[36] Lima, R., Seabra, A.B. and Durán, N. (2012) Silver Nanoparticles: A Brief Review of Cytotoxicity and Genotoxicity of Chemically and Biogenically Synthesized Nanoparticles. *Journal of Applied Toxicology*, **32**, 867-879. https://doi.org/10.1002/jat.2780

[37] Abbas, F., Iqbal, J., Jan, T., Sajjad, M., Gul, A., Abbasi, R., Mahmood, A., Ahmad, I. and Ismail, M. (2015) Differential Cytotoxicity of Ferromagnetic Co Doped CeO Nanoparticles against Human Neuroblastoma Cancer Cells. *Journal of Alloys and Compounds*, **648**, 1060-1066. https://doi.org/10.1016/j.jallcom.2015.06.195

[38] Khan, S., Anees, A., Ansari, A.A., Ahmad, R., Al-Obaid, O. and Al-Kattan, W. (2015) *In Vitro* Evaluation of Anticancer and Antibacterial Activities of Cobalt Oxide Nanoparticles. *Journal of Biological Inorganic Chemistry*, **20**, 1319-1326. https://doi.org/10.1007/s00775-015-1310-2

[39] Gopinath, K., Chinnadurai, M., Devi, N.P., Bhakyaraj, K., Kumaraguru, S., Baranisri, T., Sudha, A., Zeeshan, M., Arumugam, A., Govindarajan, M., Alharbi, N.S., Kadaikunnan, S. and Benelli, G. (2017) One-Pot Synthesis of Dysprosium Oxide Nano-Sheets: Antimicrobial Potential and Cyotoxicity on A549 Lung Cancer Cells. *Journal of Cluster Science*, **28**, 621-635. https://doi.org/10.1007/s10876-016-1150-4

[40] Arbab, I.A., Abdul, A.B., Sukari, M.A., Abdullah, R., Syam, S., Kamalidehghan, B., Ibrahim, M.Y., Taha, M.M.E., Abdelwahab S.I. and Ali, H.M. (2013) Dentatin Isolated from Clausena Excavate Induces Apoptosis in MCF-7 Cells through the Intrinsic Pathway with Involvement of NF-*k*B Signalling and G0/G1 Cell Cycle Arrest: A Bioassay-Guided Approach. *Journal of Ethnopharmacology*, **145**, 343-354. https://doi.org/10.1016/j.jep.2012.11.020

[41] West, J.L. and Halas, N.J. (2000) Applications of Nanotechnology to Biotechnology, *Current Opinion in Biotechnology*, **11**, 215-217. https://doi.org/10.1016/S0958-1669(00)00082-3

[42] Alphandary, P.H., Andremont, A. and Couvreur, P. (2000) Targeted Delivery of Antibiotics Using Liposomes and Nanoparticles: Research and Applications. *International Journal of Antimicrobial Agents*, **13**, 155-168. https://doi.org/10.1016/S0924-8579(99)00121-1

[43] Cleveland, J.L. and Kastan, M.B. (2000) Cancer—A Radical Approach to Treatment.

Nature, **407**, 309-311. https://doi.org/10.1038/35030277

[44] Khana, S., Al-Ansaric, A., Rolfod, C., Coelhod, A., Abdullae, M., Khayale, K.A. and Ahmade, R. (2017) Evaluation of *in Vitro* Cytotoxicity, Biocompatibility, and Changes in the Expression of Apoptosis Regulatory Proteins Induced by Cerium Oxide Nanocrystals. *Science and Technology of Advanced Materials*, **18**, 364-373. https://doi.org/10.1080/14686996.2017.1319731